# Improved Performance of Reduced Silver Substrates in Surface Enhanced Raman Scattering

**Salman Daniel**

**242723**

ITÄ-SUOMEN YLIOPISTO

**Master Thesis**

**March 2013**

**Department of Physics and Mathematics**

**University of Eastern Finland**

**Salman Daniel** *Improved Performance of Reduced Silver Substrates in Surface Enhanced Raman Scattering*

University of Eastern Finland

Master's Degree Programme in Photonics

Supervisors Prof. Pasi Vahimaa

Prof. Jari Turunen

---

## Abstract

Reduced silver substrates play a significant role in surface enhanced Raman scattering (SERS). In this work, we study the performance of a silver colloidal solution as an active-medium for SERS measurements which produces a uniform surface area. Two different silver colloidal solutions are prepared through wet chemistry techniques. Different materials are used as substrates in SERS measurements, and it is found that polycarbonate and cyclo olefin copolymer substrates are effective as they produce considerably enhanced Raman signal in comparison with other substrates such as silver, copper, $TiO_2$ in amorphous and crystalline form, and $SiO_2$. Further enhancement in the Raman signal of rhodamine 6G (Rh6G) molecules is obtained by employing periodically one and two dimensional modulations combined with reduced silver particles on the surface of cyclo olefin copolymer substrate. It is examined that periodically one dimensional modulation are more advantageous in producing enhanced Raman signal.

# Acknowledgements

Foremost, thanks to God Almighty through Him everything is possible. I am deeply indebted to my supervisors Prof. Pasi Vahimaa (Head of Department) and Prof. Jari Turunen for their guidance and encouragement to carry out this research work at department of Physics and Mathematics. I am thankful to Jussi Rahomäki and Tarmo Nuutinen for their assistance in preparation of samples and using wet chemistry techniques respectively. Last but not least, I am grateful to my family members specially my mother for her prayers and infinite love.

Joensuu, March 22, 2013. *Salman Daniel*

# *Contents*

# 1. Introduction

Interaction of light with matter produces several significant phenomena which help to understand the nature of matter. One of those light-matter interaction phenomena is scattering of photons e.g. Surface Enhanced Raman Scattering (SERS). The SERS can be summarized as an amplification of Raman signal by several orders of magnitude when the interaction of electromagnetic light occurs with metals which produce plasmon resonance [1].

The first ever reported observation of the SERS effect was presented by Fleischmann et al., [2] in 1974, while doing the work on pyridine on electro-chemical roughened silver electrodes. At that time it was believed that signal enhancement is because of the larger surface area. Later on, in 1977, an interesting finding was reported claiming a flat surface to give Raman enhancements in the range of $10^3$-$10^6$. This was the beginning of Surface Enhanced Raman spectroscopy. The studies by Jeanmaire and Van Duyne, and Albrecht and Creighton negated the reason of signal enhancement by an increased surface area [3, 4].

A plasmon resonance is a core process in SERS and mostly silver (Ag) and gold (Au) metals are used as substrates because of the occurrence of surface plasmon resonance in the visible region. Metals like Al, Ga, In, Pt, Rh, metal alloys and alkali metals (Li, Na, K, Rb and Cs) can also be used as substrates in SERS but enhancement is low as compared to Ag and Au. One can also use semiconductors, quantum dots and graphene as substrates which provide a significant enhancement factor in SERS measurements [5].

Surface enhanced Raman scattering (SERS) is a vast field of study and touches the boundaries of physics, chemistry, biology and nano-science because of its inter-disciplinary nature. The benefits of SERS detection are high sensitivity, a provision of a high specificity and the unique fingerprint of the molecule spectra which gives a birth of its most potential applications in analytical chemistry, biochemistry, forensic sciences, trace analysis of drugs, explosives, and also for glucose sensing or monitoring [6]. Detection and identification of dyestuffs from old artwork like paintings and medieval manuscript is also possible through SERS [7-9].

Surface enhanced Raman scattering is a rapidly growing field of study even at its entrance in the fourth decade. In recent years, citation data in Web of Science for the term “Surface enhanced Raman” has touched the rim of 30000 publications. Furthermore, in the field of medical study spectroscopy of single hemoglobin molecules, cancer gene detection and optical tags are becoming possible through SERS [10-12]. Some other applications in the field of biology where SERS leads from the front are included the detection of glucose, pathogen, biological toxins and intracellular [13-16]. There are several other advantages of surface enhanced Raman spectroscopy which makes it use easy in a variety of applications such as it is a non-destructive and non-invasive technique which can work in-situ and in-vitro for biological samples under a wide range of conditions. Surface enhanced Raman spectroscopy provides a possibility to detect a single DNA base [17]. An important feature of SERS is that, in principle, it can work at any excitation wavelength and provides a scope for improved photo-stability.

There are many aspects which have contributed to enhance the interest in SERS. For instance, the dramatic developments of nano-science and nanotechnologies, as well as a rapid increase of research in the field of plasmonics have opened the new horizons in science. On the other hand, improvements in Raman instrumentation have made the technique available for a wider community of scientists as well as its inter-disciplinary nature has stimulated the field [18, 19].

The important areas of research and applications which are contributing to SERS are electro-chemical studies, surface enhance hyper-Raman, electromagnetic enhancements at hot-spots, resonance and polarization effects, single molecule spectroscopy, tip-enhancement Raman scattering, development of novel analytes and isotropic editing of SERS probes, and substrate development with the advent of nanotechnologies [1]. Recently the spatial resolution of Raman measurements is studied through the observation of the SERS spectrum of a single molecule by the coupling of the Raman spectroscope with the scanning probe microscope [20]. A deep UV SERS would be useful for investigating biological molecules, but it is necessary to find suitable metals as plasmonic materials as well as take care of photo-degradation of samples. Recently Aluminum (Al) and Al coated Si tip has provided significant enhancement in SERS [21]. Highly resolved structural information on the femtosecond timescale can be obtained through Femtosecond Stimulated Raman Spectroscopy (FSRS), which is a coherent and stimulated vibrational technique [22].

In recent years several different SERS enhancement geometries were employed to achieve a good enhancement from the probe. In 1996 Garcia-Vidal and Pendry used the concept of the collection of closely spaced semicylinders on a flat surface and produced a highly localized field between the two metallic surfaces [23]. Regular arrays of isolated metallic nanoparticles on a metal film substrate were characterized using far-field Raman spectroscopy and localized surface plasmon resonance was observed between the particles [24, 25]. Metallic nanoshells geometry can be used to reduce plasmon linewidths at near-infrared frequencies. Aligned high-aspect silver nanowires, which were fabricated through a porous alumina template, are used to SERS detection [26]. A highly enhanced field was observed at the sharp tip of metal nanoparticles which were fabricated in the form of a crescent moon due to localized plasmon resonances and the lightning rod effect [27]. Baumberg et al., 2005 employed nanovoid lattice in flat metal film structured which were useful to support localized plasmon resonances [28].

Often the SERS geometries are the consequences of nanotechnologies which are expensive and time consuming processes. We have employed metallic nanoparticles of silver (Ag) in solution (colloidal solution) as an active-medium and different materials such as $TiO_2$ in the amorphous and crystal form, cyclo olefin copolymer (COC), polycarbonate (PC), silver (Ag), copper (Cu) and $SiO_2$ are used as substrates to study the SERS spectrum of rhodamine 6G (Rh6G) molecules. Surface enhanced Raman spectroscopy is proceeded in a quest to find out the performance of reduced silver nanoparticles as active media and Raman signal of Rh6G is analyzed by introducing artificial nanostructure modulations on COC substrate. Silver metal colloids are prepared through wet chemistry techniques which provide cost efficient fabrication methods such as chemical reduction, laser ablation and photo-reduction. We have

used Tollens and Citrate-reduced silver colloidal methods to fabricate Ag metal colloids. These are the simple fabrication approaches which provide high stability of colloids for a longer period of time, although there is a minor possibility for change in chemical properties.

This thesis is organized as follow: In Chapter two, aim and strategy of the work are presented. In Chapter three, the theory and models of surface enhanced Raman scattering are discussed. Chapter four contains fabrication and experimental set-up of the work. Results and discussion are presented in Chapter five, while the conclusion part is presented in Chapter six.

# 2. Aim and strategy of the work

In this chapter, the aim and strategy of our work are discussed which will encourage the reader to move forward in the details of the work.

## 2.1 AIM OF THE WORK

The main goal of this work is to improve the performance of reduced silver substrates in surface enhanced Raman scattering. We would try to find a silver colloidal solution as an active-medium for SERS which provides most uniform surface and enhanced Raman signal. Furthermore, the capability of different materials such as $TiO_2$ amorphous and crystal form, cyclo olefin copolymer (COC), polycarbonate (PC), silver (Ag), copper (Cu) and $SiO_2$ surfaces as substrates would be tested through the analysis of a SERS spectrum of rhodamine 6G molecules. Finally, artificial surface modulations combined with Ag colloids are employed on COC substrate to observe whether it benefits the Raman signal or not.

## 2.2 STRATEGY

In quest to achieve our aim, we would use two different fabrication methods to prepare silver colloidal solution. One fabrication method is a Tollens method which is a one step process and produces silver nanoparticles in the range of 50 nm – 200 nm [29]. The other method is a Citrate-reduced colloidal solution method. The silver colloidal solution prepared by the Citrate-reduced method is distributed into different fractions according to different sizes of silver nanoparticles through a centrifugation. These fractions with reducing order of particle sizes are named as 1, P1, P2, P3 and P4. Silver nanoparticles prepared by these two methods are used as active-media for SERS on the surfaces of $TiO_2$ in amorphous and crystal form, cyclo olefin copolymer (COC), polycarbonate (PC), silver (Ag), copper (Cu) and $SiO_2$ substrates. The strategy to achieve our goal is shown in Fig. 1.

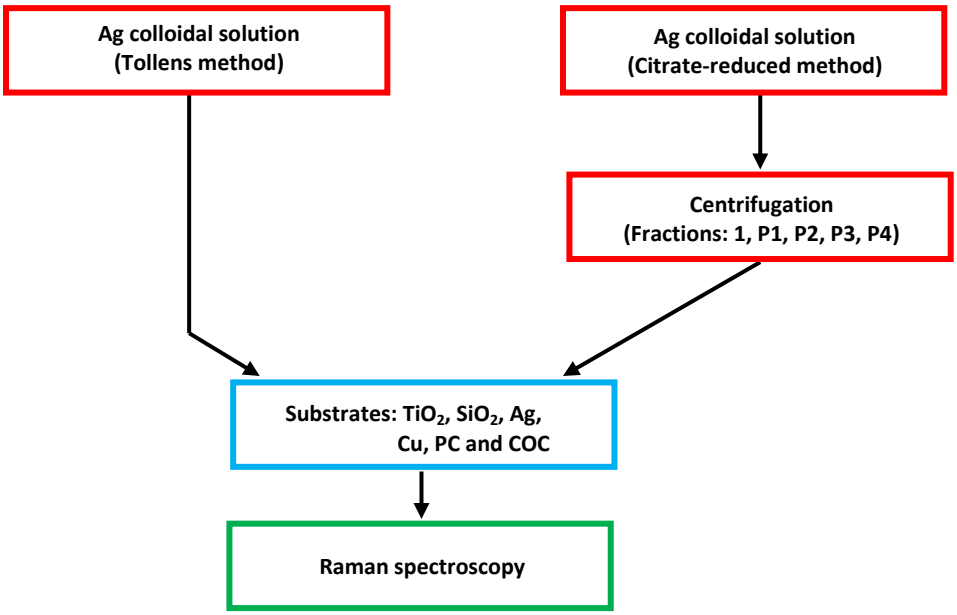


**Figure 1**. Schematic diagram representing plan of action followed to achieve our aim.

Then artificial modulations (one and two dimensional) are employed on the surface of COC substrate. This modulated substrate combined with silver colloidal solution prepared by the Citrate-reduced method is used to observe further enhancement in Raman signal. Schematic diagram is shown in Fig. 2.

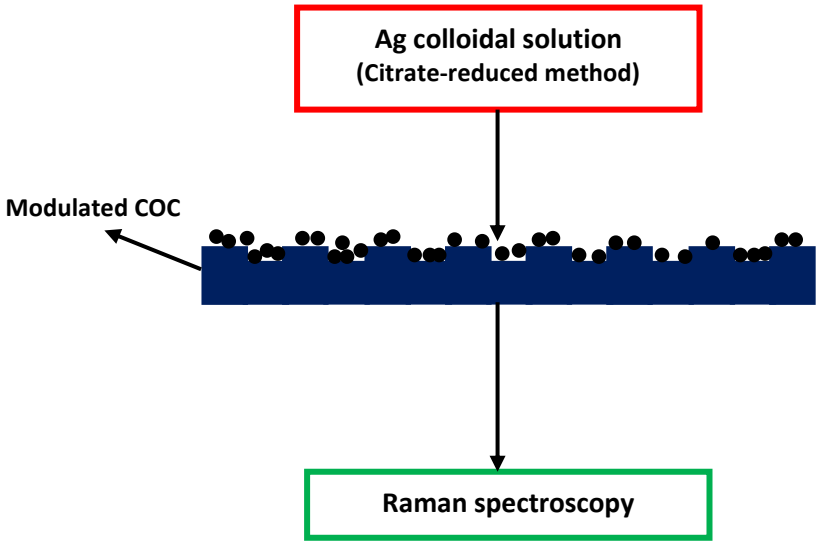


**Figure 2.** Schematic diagram of Raman spectroscopy using Ag colloidal solution on the surface of modulated COC

# *3. Theory of surface enhanced Raman scattering*

In this chapter the theory of Raman scattering as well as theoretical models for the Raman enhancement, including metallic nanosphere and charge-transfers models, are discussed.

## 3.1 RAMAN SCATTERING

Raman scattering was discovered by Chandrasekhara Venkata Raman in Sub-continent (British India) in the year of 1921 using the sun as a light source and his eyes as a detector. He observed the change in scattered light with respect to the incident light in several organic liquids and today we call it Raman effect or Raman scattering [30]. Inelastic scattering involves transitions between the vibrational or rotational levels in molecules. The measurement and analysis of the Raman effect are called as Raman spectroscopy.

The interaction of light with a molecule makes a change in electronic energy levels through the movement of electrons or in the motional energy states of an atom in the molecule. In the following couple of paragraphs a brief introduction of the electronic states, motional states and transitions between the molecular states is presented to understand the phenomenon of light-matter interaction.

### 3.1.1 Electronic and vibrational states

When electrons occupy a lower energy state and obey Pauli's exclusion principle it corresponds to the ground electronic state. All electrons in the ground state exist in pairs and contain an opposite spin. Electrons total spin is zero in the ground state which is known as a singlet state. The electron is transferred from the ground to an excited state and it breaks the Pauli's exclusion principle. Rotation of a molecule or vibration of atoms in the molecule makes a small perturbation into the electronic state. Consequently, one can divide the electronic states into vibrational states which contain small energies in comparison with the electronic states as it is shown in Fig. 3.

Transitions between the molecule's states occur in the form of absorption or the loss of energy. If the transition occurs between two different electronic states, it is known as an electronic transition and in the case of two different vibrational states, it is called as a vibrational transition. In these transitions if absorption or an emission of a photon is involved then it is a radiative transition. Sometimes only a relaxation from an excited vibrational state to the ground vibrational state occurs which is known as a non-radiative transition.

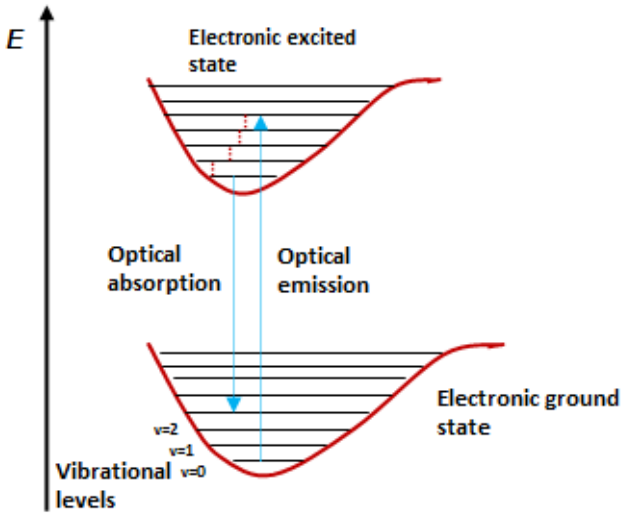


**Figure 3.** Schematic diagram of electronic and vibrational states in a molecule.

### 3.1.2 Fluorescence and scattering processes

Fluorescence which contributes significantly in SERS occurs when an electron is excited and jumps to an excited electronic state, then it relaxes down in vibrational excited states and finally jumps back to the ground electronic state with an emission of a photon. Fluorescence is a two-steps process which provides information about the electronic and vibrational structure of a molecule. On the other hand, scattering is a simultaneous process of absorption of an incident photon and emission of another photon. It can be further divided into two processes: (a) an elastic scattering in which a molecule comes back to the initial energy state after the scattering while incident and scattered photons have the same amount of energy and it is known as Rayleigh scattering. In the other process (b), the scattered photon has a different amount of energy than that of the incident photon. It is called as an inelastic scattering which involves a transition between vibrational states of the molecule which is known as Raman scattering. These three types of phenomena fluorescence, elastic and inelastic scattering are shown in Fig. 4 below where $E_{in}$ and $E_s$ represent incident and scattered photon energies respectively. A virtual state is showing a mathematical construction of the perturbation theory without any physical meaning and it is more related to quantum physics which is out of the scope of this work.

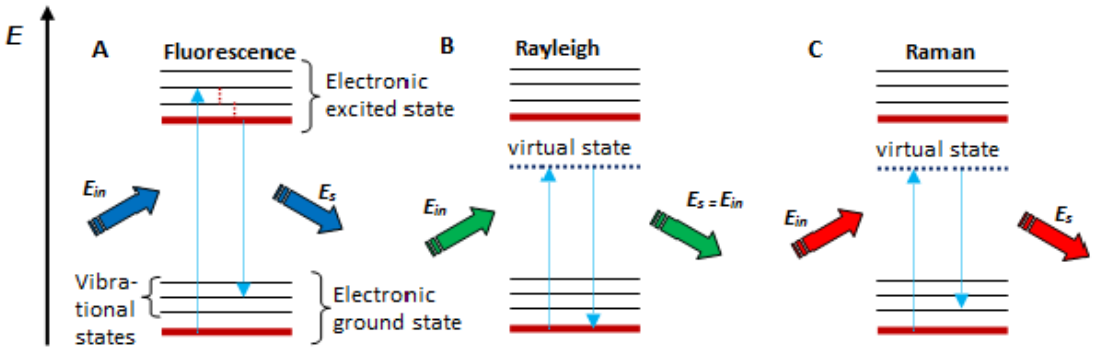


**Figure 4.** Jablonski diagram of (A) fluorescence (B) Rayleigh and (C) Raman scattering.

Usually an inelastic scattering is classified into two different processes on the basis of scattered photon energy. These processes are known as Stokes and anti-Stokes which are discussed below.

### 3.1.3 Stokes and anti-Stokes processes

In the Stokes process a photon of a certain amount of energy $E_{in}$ interacts with a molecule which is relaxed in its electronic ground state, and makes a shift of an electron from ground level to a virtual level. The electron jumps back to the first excited state of a vibrational mode with a scattered photon of energy less than that of the incident photon.

Anti-Stokes process is an opposite of Stokes process. In this process a molecule is already in the first excited state of vibrational mode and it turns to the vibrational ground state through a scattered photon of higher energy than that of the incident photon. Both processes are explained with the help of Jablonski diagram in Fig. 5 below.

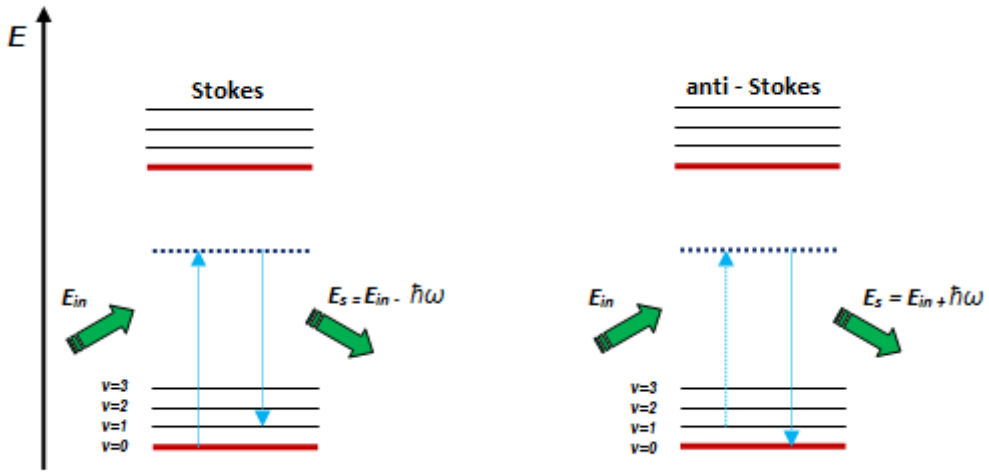


**Figure 5.** Jablonski diagram of Stokes and anti-Stokes scattering processes.

## 3.2 OPTICAL PROPERTIES OF SILVER NANOPARTICLES

Nanoparticles which have diameter in the range of 10 nm – 200 nm depict interesting phenomena because of their large surface to volume ratio. For example, an excitation of plasmon resonance makes them valuable in several applications in the field of spectroscopy, optoelectronics and optical waveguides [31, 32]. Ag nanoparticles have properties such as a high ability of resistance to oxidation, and their optical cross-section is five times larger than that of gold nanoparticles of the same size [33]. They also have unique optical properties which are the consequences of collective oscillations of conduction electrons by the incident electric field. These optical properties depend on the size, shape and local dielectric environment of nanoparticles.

The origin of these unique properties of Ag nanoparticles is the presence of free conduction electrons. A neutral medium with the equal concentration of free-electrons with heavier ion cores can be used to study the optical properties of the metals. This medium is known as plasma. The optical response of plasma can be understood by constructing a model through keeping in mind that electrons have interactions with ions, impurities, phonons, fermionic nature of electron and interaction with other electrons. Here we present a simple model which provides help to understand the optical properties of metals named as the Drude model.

### 3.2.1 The Drude model

Electrons get acceleration on applying an electric field on plasma of free-electrons and heavier positive ions [34]. When electrons move, they collide with other electrons, impurities and ions. As a result of these interactions, electrons lose a small part of their velocity i.e. the higher the velocity the higher the probability to strike with other electrons. It is a classical approach and one can write the force experienced by an electron using the following equation:

$$m\frac{d^2x}{dt^2} + m\gamma\frac{dx}{dt} = -eE(t), \tag{1}$$

where $m$, $\gamma$ and $E(t)$ represent electron mass, damping factor and incident electric field respectively. In case of monochromatic field, one can write Eq. (1) as:

$$m\frac{d^2x}{dt^2} + m\gamma\frac{dx}{dt} = -eE_0\exp(i\omega t), \tag{2}$$

where $x(t) = x_0\exp(i\omega t)$.

Electric polarization can be written as:

$$P(t) = -Nex(t). \tag{3}$$

In Eq. (3), $N$ represents the number of electrons per unit volume. Using an equation of total flux density, one can determine relative dielectric constant $\varepsilon_r$.

$$D(t) = \varepsilon_0 E(t) + P(t) = \varepsilon_0 E(t) - \frac{Ne^2}{m(\omega^2 - i\omega\gamma)} E(t) = \varepsilon_0 E(t)\varepsilon_r, \quad (4)$$

$$\varepsilon_r(\omega) = 1 - \frac{Ne^2}{m\varepsilon_0(\omega^2 - i\omega\gamma)} = 1 - \frac{{\omega_p}^2}{\omega^2 - i\omega\gamma}. \quad (5)$$

In Eq. (5), $\omega_p$ represents plasma frequency and can be defined as:

$$\omega_p = \left(\frac{Ne^2}{m\varepsilon_0}\right)^{\frac{1}{2}}. \quad (6)$$

If we assume that damping factor is zero then dielectric constant can be written as:

$$\varepsilon_r(\omega) = 1 - \frac{{\omega_p}^2}{\omega^2}. \quad (7)$$

Now considering the situation when $\omega_p = \omega$, then uniform displacement of the whole electron gas with respect to ion cores will take place. Ion cores will exert a restoring force to oppose the displacement of electrons and as a result electrons will start oscillations corresponding to ion cores. It is shown in Fig. 6. These oscillations are known as volume plasmons which are purely longitudinal and impossible to couple to transverse electromagnetic waves. The quantum of these collective plasma oscillations is called a plasmon which was first introduced by Pines in 1956 [35]. The oscillations of surface charge density fluctuations are possible at the surface of solids, propagating at the interface between a metal and a dielectric material. These kinds of oscillations are known as surface plasmon polaritons.

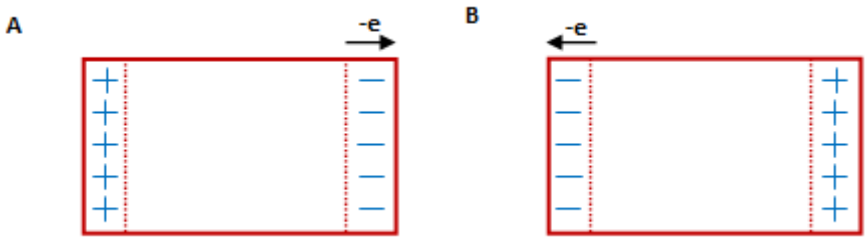


**Figure 6.** Plasma oscillations of free electrons according to Drude model.

In case of noble metals like silver and gold, at $\omega > \omega_p$ interband transitions occur, which make electrons excited to the higher bands and lead to increase in imaginary part of dielectric constant [34]. Therefore, one needs to modify Eq. (2) and write it down as:

$$m\frac{d^2x}{dt^2} + m\gamma\frac{dx}{dt} + m\omega_0^2 x = -eE_0\exp(i\omega t), \quad (8)$$

where $\omega_0$ represents the frequency of a bound electron.

### 3.2.2 Localized surface plasmon resonance

When the collective oscillations of free-electrons exist between metal/dielectric interface it is usually known as surface plasmon. The situation comes when an incident field in resonant with surface plasmon and collective oscillations start propagating in metal/dielectric interface it is known as plasmon-polaritons. In the case of localized surface plasmon resonance, surface plasmon exists in resonance with an incident field and limits in a volume of nanoparticles. It produces a large localized field in the vicinity of a particle which plays a significant role in surface enhanced Raman scattering to enhance a signal. The localized field in the vicinity of nanoparticle is shown in Fig. 7. The electrons' density is polarized corresponding to the incident field and start oscillations. One can find the resonance condition employing scattering and absorption spectroscopy which depends on the size and shape of the particles.

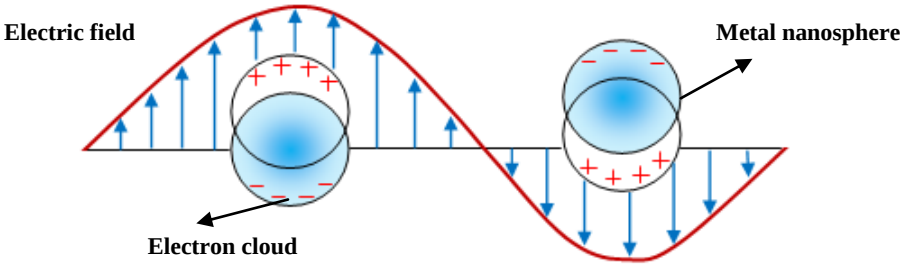


**Figure 7.** Schematic diagram of localized surface plasmon resonance (LSP).

One can find the field distribution around a spherical nanoparticle using electrostatics. Consider a homogeneous external electric field $E_e$ oriented along $z$-axis, incident on a spherical nanoparticle as shown in Fig. 8, where $a$ and $r$ represent the radius of the particle and position vector a point $P$ respectively, while $\varepsilon_{in}$ and $\varepsilon_{out}$ represent dielectric function of a sphere nanoparticle and dielectric constant of the surrounding medium respectively. The total electric potential can be written as:

$$\Phi_{out} = \left(\frac{\varepsilon_{in} - \varepsilon_{out}}{\varepsilon_{in} + 2\varepsilon_{out}}\frac{a^3}{r^3} - 1\right) E_e z. \tag{9}$$

$$\Phi_{in} = -\left(\frac{3\varepsilon_{out}}{\varepsilon_{in} + 2\varepsilon_{out}}\right) E_e z. \tag{10}$$

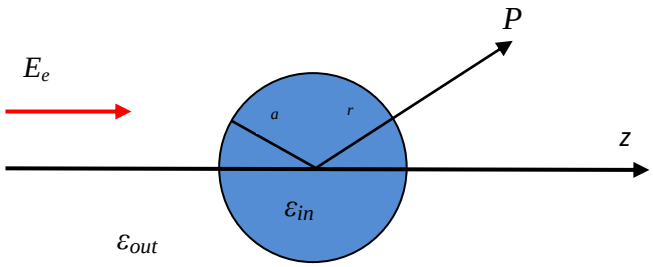


**Figure 8.** Interaction of a homogeneous external field with a spherical nanoparticle.

The internal field $E_{in}$ inside the particle is calculated using this relation:

$$E_{in} = -\frac{d\Phi_{in}}{dz} = \frac{3\varepsilon_{out}}{\varepsilon_{in} + 2\varepsilon_{out}} E_e, \tag{11}$$

$$\frac{E_{in}}{E_e} = \frac{3\varepsilon_{out}}{\varepsilon_{in} + 2\varepsilon_{out}}. \tag{12}$$

The high field around a particle can be achieved if $\varepsilon_{in} + 2\varepsilon_{out} = 0$, or $\varepsilon_{in} = -2\varepsilon_{out}$, so it requires one "ε" be negative. It is known as a Fröhlich condition which corresponds to a dipolar localized surface plasmon resonance (LSPR) [34].

In a case when a spherical nanoparticle is in the air ($\varepsilon_{out}$=1), Eq. (12) can be written as:

$$E_{in} = \frac{3}{\varepsilon_{in} + 2}. \tag{13}$$

Therefore, the polarization in the sphere can be determined as

$$P = \varepsilon_0 \chi E_{in} = \varepsilon_0(\varepsilon_{in} - 1)\frac{3}{\varepsilon_{in} + 2} E_e, \tag{14}$$

and the corresponding dipole moment will be written as

$$\mu = V_{NP} P = \frac{4}{3}\pi R^3 \frac{3\varepsilon_0(\varepsilon_{in} - 1)}{\varepsilon_{in} + 2} E_e, \tag{15}$$

where $V_{NP}$ and $R$ are the volume and radius of the spherical nanoparticle respectively. Equation (15) leads to an isotropic polarization as:

$$\alpha = \frac{\mu}{E_e} = 4\pi\varepsilon_0 R^3 \frac{(\varepsilon_{in} - 1)}{\varepsilon_{in} + 2}. \tag{16}$$

Similarly, one can determine the polarizability for ellipsoidal particles and it is written as:

$$\alpha = \frac{4}{3}\pi\varepsilon_0 R^3 \frac{\varepsilon_{in} - \varepsilon_{out}}{\varepsilon_{out} + L(\varepsilon_{in} - \varepsilon_{out})}, \tag{17}$$

where $L$ is the shape factor which has values between 0 and 1 and can be calculated analytically. Mie used Maxwell's equations to find the scattering and extinction efficiencies for a homogeneous sphere [36]. When the Fröhlich condition is fulfilled both scattering and absorption are enhanced at the dipole particle plasmon resonance for metal nanoparticles. Therefore, extinction increases too which in the case of much smaller spherical nanoparticle as compared to the wavelength of the incident light can be expressed as:

$$Q_{ext} = 9\frac{\omega}{c}V\varepsilon_{out}^{3/2} \times \frac{\varepsilon_2(\lambda)}{[\varepsilon_1(\lambda) + 2\varepsilon_{out}]^2 + \varepsilon_2(\lambda)^2}, \tag{18}$$

where $V, \lambda$ and $\varepsilon_{out}$ represent the volume of the nanoparticle, a wavelength of light and the dielectric constant of the surrounding media respectively, while $\varepsilon_{in}(\lambda)$ is the complex dielectric form of metal which depends on the wavelength of light and can be written in real and imaginary form as $\varepsilon_1(\lambda) + i\varepsilon_2(\lambda)$. Therefore, any change in the dielectric constant of the surrounding medium shifts the plasmon resonance.

### 3.3 ELECTROMAGNETIC AND CHEMICAL ENHANCEMENTS

To understand the concept of the enhancement in Raman signal we first construct a system, which usually consists of a layer of metal nanoparticles acting as an active-medium for SERS, molecules are placed on a layer of metal nanoparticles acting as a probe and a substrate. It is shown in Fig. 9 below.

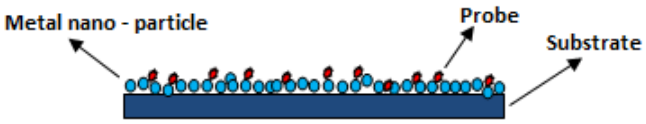


**Figure 9.** Schematic diagram metal nano-particles, probe (molecules) and substrate for Raman spectroscopy.

When the incident light interacts with particles it polarizes them, makes the conduction electrons excited and ultimately induces excitation of surface plasmons. Molecules on the surface of nanoparticles are influenced by large local fields, polarized and in a response Raman signal enhancement occurs. This phenomenon is known as the electromagnetic enhancement effect. The field caused by excitation of surface plasmon decreases as $1/r^3$ on moving away from the surface where $r$ represents the distance. Therefore, a probe should be located close to the surface as it is influenced by enhanced local field and get polarized. The other enhancement effect of Raman signal is known as a chemical effect. The polarizability of a molecule is affected because of interaction between the probe and the metal surface.

There are several electromagnetic models for SERS presented in the previous study on SERS which provide significant assistance to understand the enhancement phenomenon through the electromagnetic effect. In our work, the model of a metallic nanosphere is discussed briefly. Other models for concentric spheres, prolate spheroids and ellipsoids, lightning rod effect, the image effect and Fresnel reflection effects can be found in Refs. [37-41].

### 3.3.1 Model of metallic nanosphere

In this model a particle size is smaller than the wavelength of incident light which is known as Rayleigh approximation condition. One can describe an effective electric field $E_e$ mathematically according to Rayleigh approximation as:

$$E_e = \frac{1}{1 + [(\varepsilon(\lambda)/\varepsilon_0) - 1]A} E_0, \tag{19}$$

where $E_0$, $\varepsilon(\lambda), \varepsilon_0$ and $A$ represent the incident field outside the particle, dielectric constant of bulk metal and the surrounding media and depolarization factor respectively. The effective field will be maximum when the denominator value in Eq. (19) goes to zero and it corresponds to resonance of surface plasmon. One can also write Eq. (19) for a small sphere as:

$$E_e = \frac{\varepsilon_{in}(\lambda) - \varepsilon_{out}}{\varepsilon_{in}(\lambda) + 2\varepsilon_{out}} E_0. \tag{20}$$

Resonance surface plasmon occurs when the real part is equal to $-2\varepsilon_0$ and the imaginary part is very small [42]. The chemical enhancement which contributes a small part in the total enhancement of Raman signal is briefly explained below through the charge transfer model and the adatom model.

### 3.3.2 Charge-transfer model

In this process probe (molecules) on the surface of nanoparticles form a chemical bond, an electron from particle shifts to the probe and make it a negative ion. It has different equilibrium geometry with respect to the original molecule. When the electron comes back to the metal particle nuclear relaxation occur, which leads to a neutral molecule through vibrational excitation and a Raman-shifted photon is emitted.

According to the adatom model the strong Raman enhancement is produced when adsorbate is located to atomic-scale roughness. Further study on the adatom model can be found in the Ref. [43]

# *4. Fabrication and experimental set-up*

In this chapter, fabrication of silver colloidal solutions through wet chemistry techniques and experimental set-up for surface enhanced Raman scattering (SERS) measurements are discussed.

## 4.1 FABRICATION METHODS

Two different methods of fabrication were used to make Ag nanoparticles in solution. The difference between these two methods and their details are discussed in the following paragraphs.

### 4.1.1 Tollens method

In Tollens method [29] 2 mL of 0.5 M fresh made silver nitrate ($AgNO_3$) added in 20 mL of dd $H_2O$ and 25% of $NH_3$ until dark precipitate appeared and finally dissolved. The final concentration of distilled water was added to get 10 mM of freshly made Tollens reagent (aqueous diamminesilver (I) complex). Tollens reagent and 1% glucose with a ratio of 40:5 were added on surfaces of $TiO_2$ crystalline and amorphous, COC and PC while heating them on a thermal block at 60°C, rinsed them with distilled water and finally dried with air. Glucose in aqueous solution provides an electron to reduce silver. Rhodamine 6G of stock 0.02% (w/v) drops added, left the surfaces to dry for 15 to 20 minutes and then dried them with air. Chemical reaction in a schematic way is shown in Fig. 10 and an ionic equation of reaction can be expressed as:

$$[Ag(NH_3)_2]^+ (aq) + e^- \rightarrow Ag\ (s) + 2\ NH_3\ (aq)$$

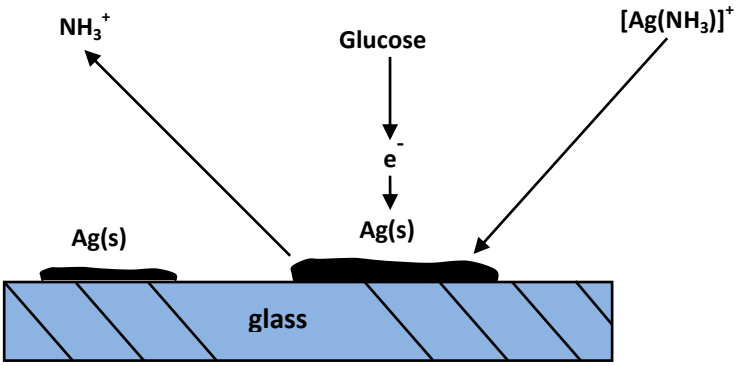


**Figure 10.** Tollens method: Reduced silver grows in islands form on a glass.

### 4.1.2 Citrate-reduced silver colloidal solution method

Silver nitrate ($AgNO_3$) of a quantity of 90 mg was dissolved in 500 mL of distilled water and brought to boiling. Sodium citrate ($Na_3C_6H_5O_7$) solution of 10 mL of 1% by weight added as a reducing and stabilizing agent. Solution was kept on boiling for an hour while refluxing the evaporating water [1]. A grey-yellow solution of 400 mL volume left remained and cooled it

down to room temperature. A schematic diagram of Citrate-reduced colloidal method can be seen in Fig. 11.

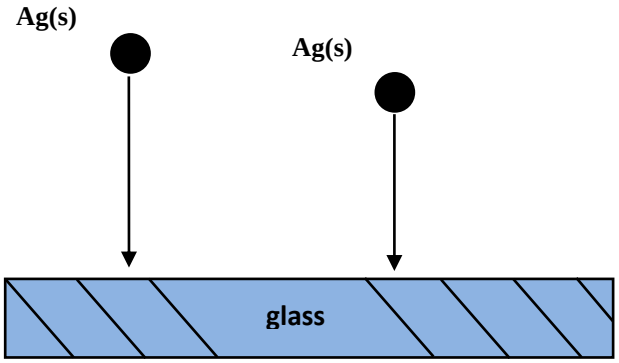


**Figure 11.** Citrate-reduced colloidal solution method: Solid silver nanoparticles settled down on a glass.

### 4.2 CENTRIFUGATION OF SILVER COLLOIDAL SOLUTION

Silver colloidal synthesized by Citrate-reduced silver colloidal method was fractioned according to different particle size distribution through the centrifugation using Eppendrof Centrifuge 5415D. Citrate reduced silver colloidal solution was centrifuged for one minute at 1000 rcf (relative centrifugal force) and pellet aggregates were discarded to get a solution of a uniform size of silver particles. Then the solution was centrifuged at 16.1×1000 rcf for 5 minutes and supernatant was discarded to get a first distribution named as #1 which contains particles of different sizes suspended in distilled water. A portion of first distribution was taken out and centrifuged at 5000 rcf for one minute to get second particles distribution named as P1. Similarly, other fractions like P2, P3 and P4 were obtained through centrifugation at 10000 rcf, 14000 rcf and 16.1×1000 rcf respectively. The whole distribution scheme of Ag colloidal solution is shown in Fig 12. A drop of 15 µl from each colloidal distribution and 2 µl of Rhodamine 6G added on the surfaces of COC and PC substrates.

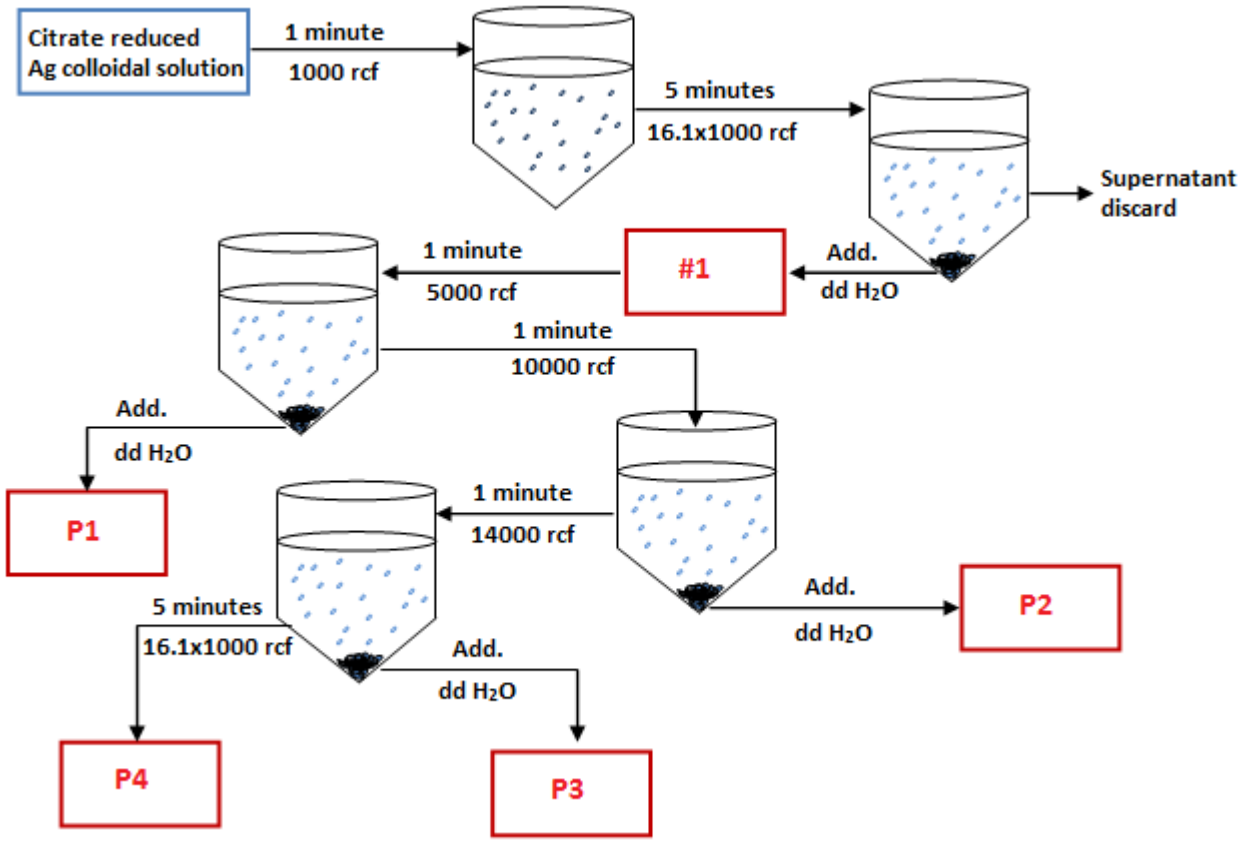


**Figure 12.** Schematic diagram showing the distribution of Ag colloidal solution through centrifugation in fractions #1, P1, P2, P3 and P4.

### 4.3 RAMAN SPECTROSCOPY

The Raman spectrum of Rh6G molecules was examined using Renishaw inVia Raman microscope while $TiO_2$ in the crystal and amorphous form, COC and PC were used as substrates. The Ag nanoparticles were used as active-media which were fabricated by Tollens method. Sixteen measurements of each sample at different points within an area of 60 µm by 60 µm were measured at the excitation wavelength of 514 nm, using power of 56 µW and the integration time of 10 seconds. Asymmetric least squares smoothing was used for baseline correction and the average Raman intensity was calculated. The Raman signal was smoothened employing Savitzky-Golay filtering method. Then the Raman spectrum of Rh6G molecules was obtained at the wavelength of 514 nm using power of 3 µW and 30 µW with integration time of 10 seconds for COC and PC substrates respectively, and Ag colloidal solution fractions named as 1, P1 and P4 were used as active-media fabricated by Citrate-reduced method.

Finally, to observe the further enhancement in Raman signal, one dimensional modulation with a period of 335 nm and line width of 125 nm, and two dimensional modulations with a period of 335 nm on both directions and feature size width of 125 nm as a grid were employed on the surface of COC. Nine spectroscopy measurements for each sample using particle distributions P1 and P4 were performed with power of 6 µW at the wavelength of

514 nm. The schematic diagrams of one and two dimensional modulations are shown in Fig. 13 below.

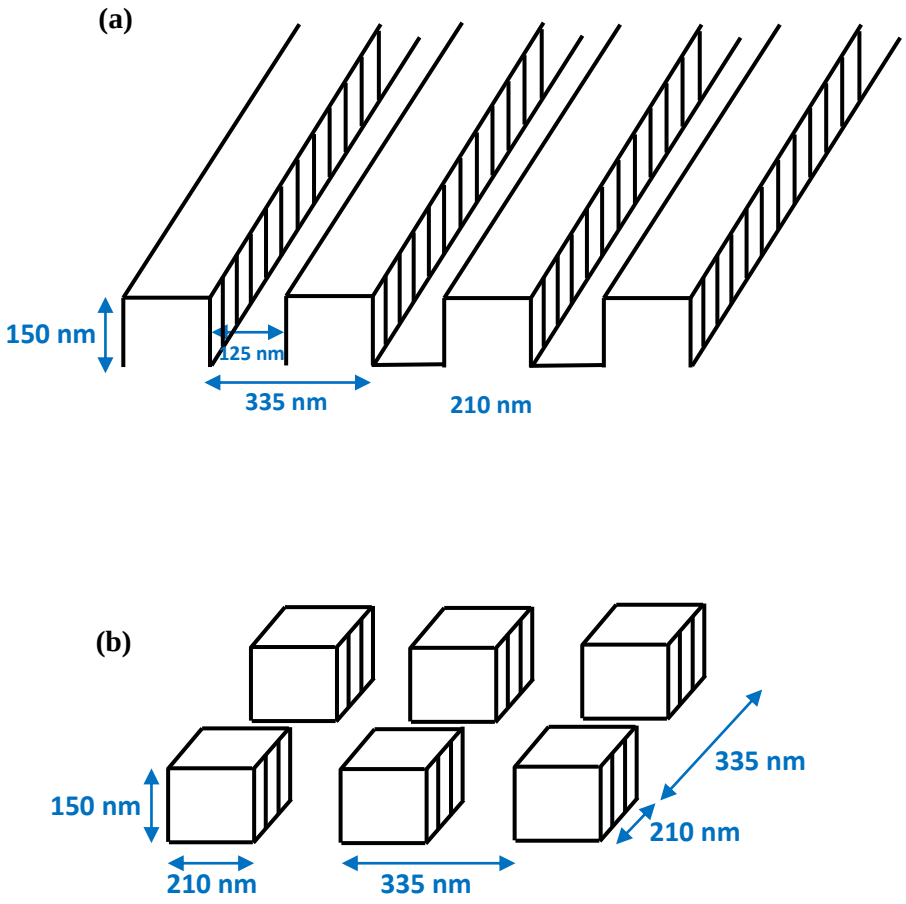


**Figure 13.**The schematic diagram of (a) one dimensional and (b) two dimensional nano-scale modulations on COC (Cyclo Olefin Copolymer) surface.

## 4.4 Experimental flow sheet

The scheme of fabrication (step-by-step) of silver colloidal solutions through Citrate-reduced and Tollen's reagent methods, as well as the preparation of the substrates for Raman spectroscopy are shown in Fig. 14.

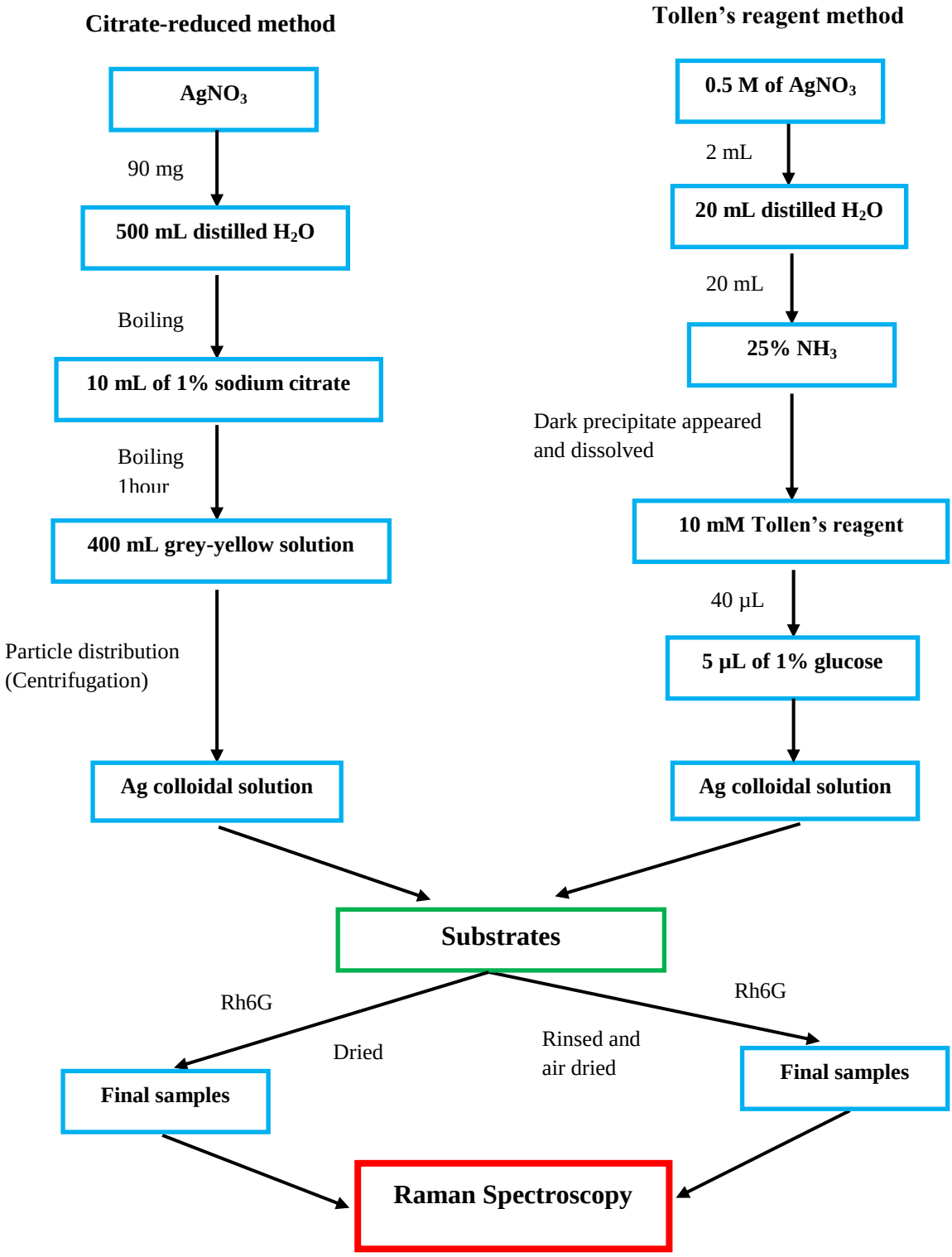


**Figure 14.** Experimental flow sheet is showing the whole scheme for SERS measurements using Citrate-reduced and Tollen's reagent method.

## 4.5 RAMAN SPECTROMETER PRINCIPLE

Raman spectrometer consists of five fundamental components (a) excitation source, (b) a microscope, (c) filter, (d) diffraction grating, and (e) a CCD camera. These components are shown in the schematic diagram of Raman spectrometer in Fig. 15. The excitation source is usually a laser which provides a coherent monochromatic beam of light. The monochromatic light confined by focusing optics excites the sample.

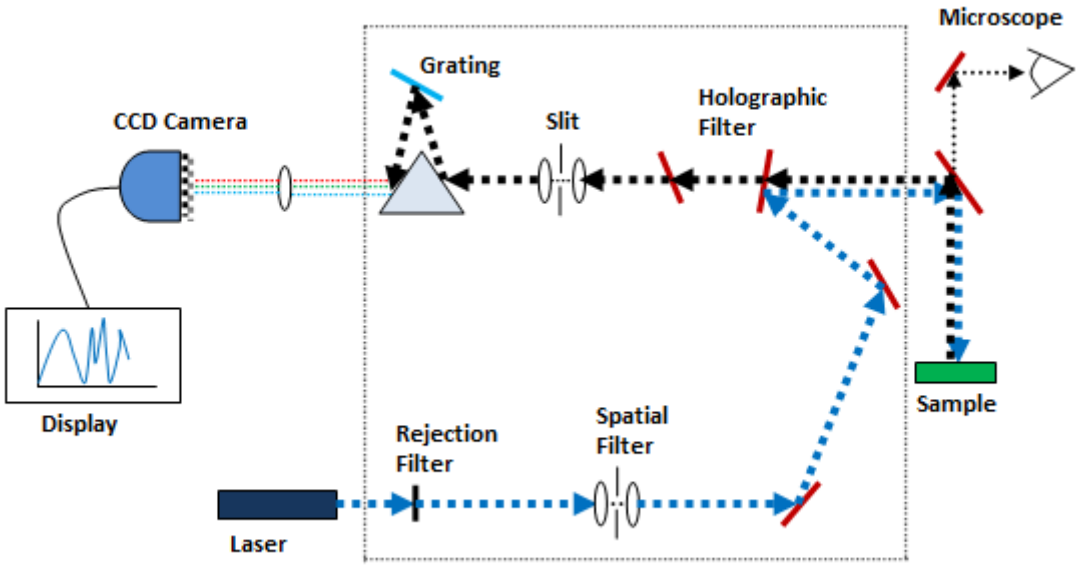


**Figure 15.** Schematic diagram of Raman spectrometer working principle.

In Raman spectrometer, the rejection filter allows the beam to pass through without any change in frequencies but attenuates those in very low levels. Spatial filter removes the aberrations from the laser beam and directs the beam to a microscope. The microscope is used to excite the sample and collects the scattered light. The scattered light passes through the holographic filter, comprising multiple superpositioned holograms which produce a filter shape with multiple peaks at specified positions as well as block the laser pump beam [44], detects the peaks in the spectrum and excitation wavelength is being filtered out. After filtering, the scattered light is sent to a spectrograph and it is separated into different wavelengths through a diffraction grating. Finally, a detector, photodiode array (PDA) or charge-coupled devices (CCD), receives scattered signals and the intensity is measured at each wavelength which is represented as a Raman spectrum on the display screen.

# *5. Results and discussion*

In this chapter the results of SERS measurements using silver colloidal solutions on non-modulated and modulated substrates are discussed.

## 5.1 SERS MEASUREMENTS USING SILVER COLLOIDAL SOLUTION SYNTHESIZED BY TOLLENS METHOD

The Raman spectrum of Rh6G molecules was obtained at power of 56 µW at 514 nm using silver colloidal solution prepared by Tollens method, and it was observed that Ag colloidal solution produces a uniform distribution on the surface of $TiO_2$ in crystal and amorphous form, and on COC substrate. The enhancement in Raman signal is higher in case of crystalline form of $TiO_2$ as it can be seen in Fig. 16. Silver nanoparticles distribution on the surface of PC substrate includes aggregation and therefore Raman signal is significantly enhanced in comparison with COC substrate. In both cases the Rh6G Raman peaks are in good agreement with the work presented by Peter Hildebrandt and Manfred Stockburger [45]. The strong bands in the range of 1300 $cm^{-1}$ to 1700 $cm^{-1}$ exist due to aromatic stretching vibrations since Rh6G contains a benzene ring structure and is charged positively. The bands in the range of 600 $cm^{-1}$ to 800 $cm^{-1}$ are the results of interaction between electronic and nuclear vibrational motion which is known as the vibronic coupling.

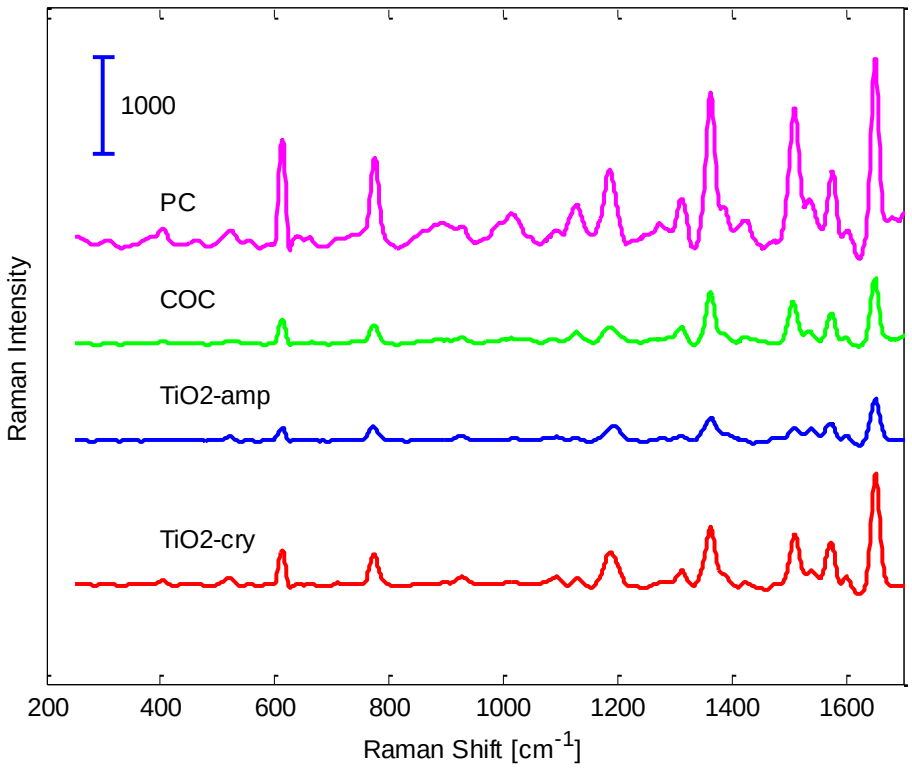


**Figure 16.** Raman peaks of Rh6G molecules using Ag colloidal solution (Tollens method) for $TiO_2$ crystalline and amorphous, PC (Polycarbonate) and COC (Cyclo Olefin Copolymer) substrates.

## 5.2 SERS MEASUREMENTS USING SILVER COLLOIDAL SOLUTION SYNTHSIZED BY CITRATE-REDUCED COLLOIDAL METHOD

The Raman signal of Rh6G molecules is much higher on COC and PC substrates due to the fractal-like colloidal aggregation of the silver nanoparticles prepared by citrate-reduced method. This aggregation produces large enhancement due to gap-plasmon resonances which consequently produce hot-spots of highly localized regions [1]. A Raman spectrum of Rh6G molecules using COC and PC substrates at the wavelength of 514 nm is shown in Fig. 15, using power of 3 µW and 30 µW respectively. Although the fractal-like colloidal aggregation has shown non-uniform structure, we chose a uniform area of 60 µm by 60 µm in size and took sixteen measurements sampled by 30 µm steps. There is not much variation in Raman signal because of the uniform distribution of nanoparticles on the surface of COC substrate using fractions 1, P1 and P4 as it can be seen in Fig. 17(a). The silver colloidal solution fraction 1 contains greater size variations of the particles and produces more SERS enhancement due to significant aggregation on PC substrate as shown in Fig. 17(b). However, the Raman intensity of Rh6G molecules is very weak for fractions P1 and P4 due to little aggregation of particles, and these are the peaks of citrate [46].

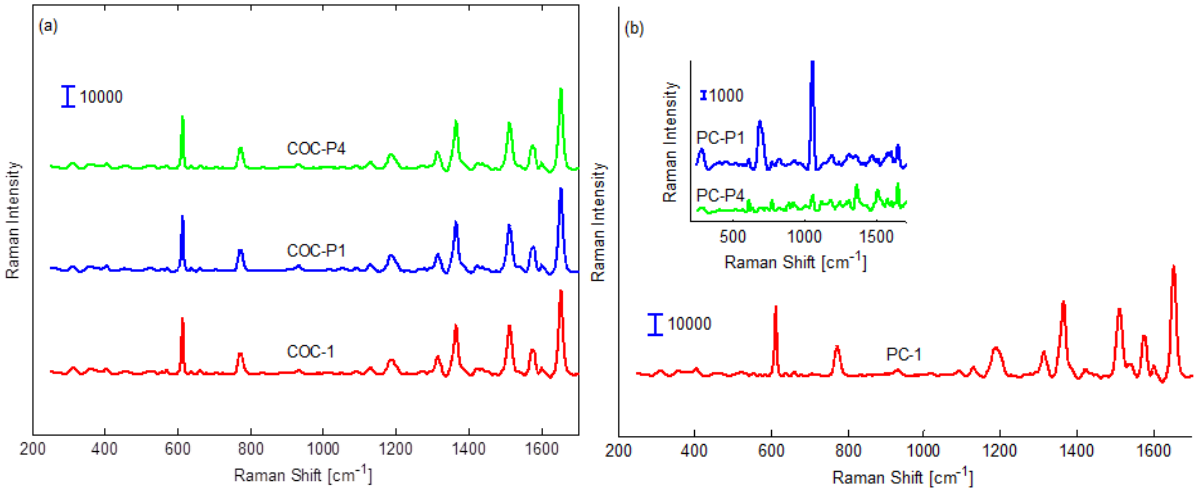


**Figure 17.** Raman spectra of Rh6G using Ag colloidal fractions 1, P1 and P4 (Citrate-reduced method) for (a) COC (Cyclo Olefin Copolymer) and (b) PC (Polycarbonate) substrates.

The variation in Raman spectrum peaks using error bars is shown in Fig. 18. The error bars show that there is no significant variation in Raman intensity for fractions 1, P1 and P4 on COC substrate as nanoparticles are distributed uniformaly and provide uniform signal over a sampling area.

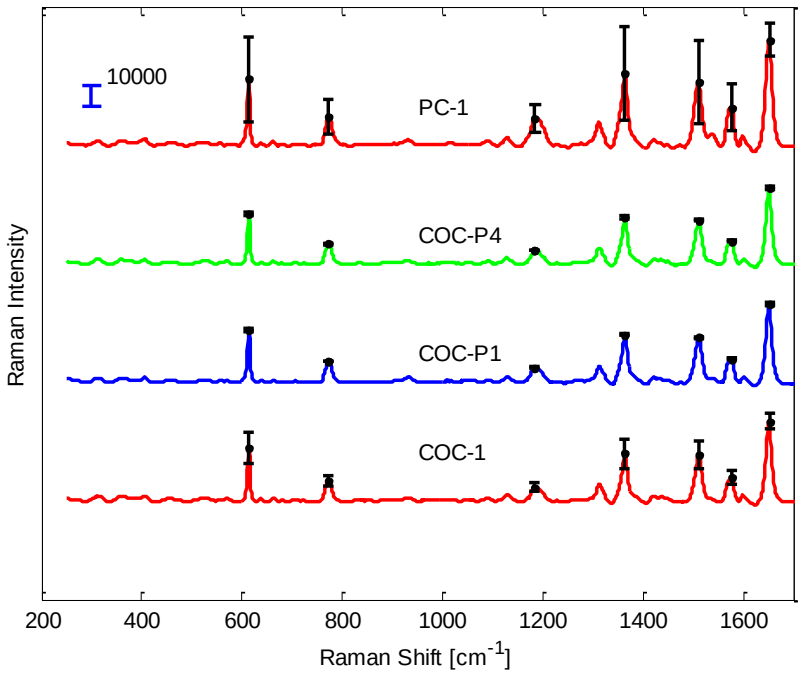


**Figure 18.** The variation in Raman peaks using error bars for Ag colloidal fractions 1, P1 and P4 on COC (Cyclo Olefin Copolymer) substrate andfraction 1 on PC (Polycarbonate) substrate.

The distribution of silver colloidal solution fractions 1, P1 and P4 on the surface of COC substrate can be seen in Fig. 19. The PC and COC substrates depict hydrophobic nature as silver nanoparticles are aggregated densely on the edges.

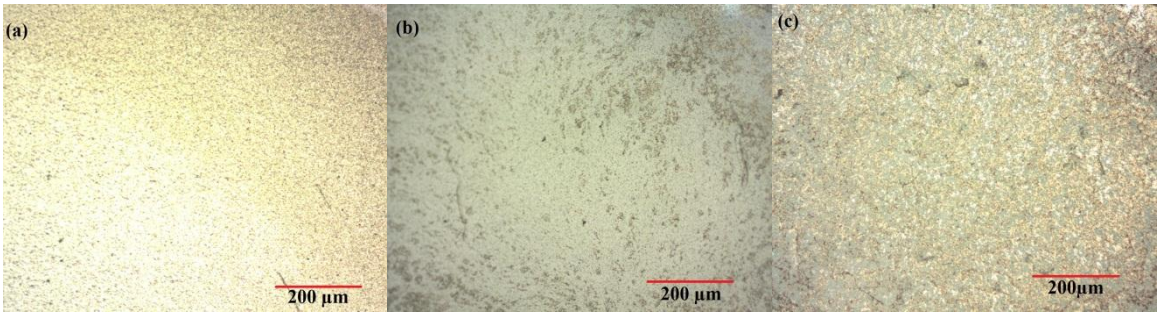


**Figure 19.** Microscope images of Ag particles distribution using fractions (a) 1, (b) P1 and (c) P4 on COC substrates.

Absorbance spectra for all silver colloidal solution fractions 1, P1, P2, P3 and P4 as well as for an orignal colloidal silver solution is shown in Fig. 20. The absorbance peak for the small size particles e.g. P4 shifts toward shorter wavelength (blue shift) and for the large size particles e.g. P1 it gets broadened and red shifted because of the dependence of plasmon band on the number of electrons present in the nanoparticle [47].

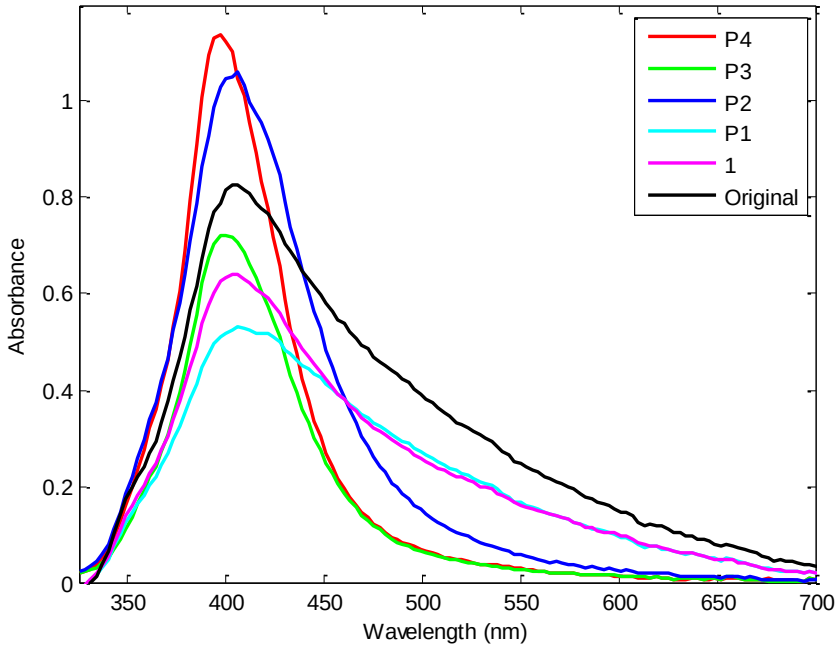


**Figure 20.** Absorbance spectra of Ag colloidal fractions 1, P1, P2, P3, P4 and original solution as well.

## 5.3 SERS MEASUREMENTS BY EMPLOYING MODULATIONS ON COC SUBSTRATE

A cyclo olefin copolymer (COC) substrate surface is modulated by making one dimensional modulation with a period of 335 nm and line width of 125 nm, and two dimensional modulations with a period of 335 nm on both directions and feature size width of 125 nm as a grid. The silver colloidal solution fraction P1 which contains more variations in particle sizes and aggregate significantly produces high enhancement in Raman signal for one dimensional modulation on COC substrate as compared to the fraction P4, which contains few silver nanoparticles, for the similar modulation. In a similar way, the signal response using fraction P4 for two dimensional modulations is weak compared to the signal from fraction P1. The average Raman intensity of nine measurements at 514 nm using power of 6 µW for fractions P1 and P4 on COC substrate is shown in Fig. 21.

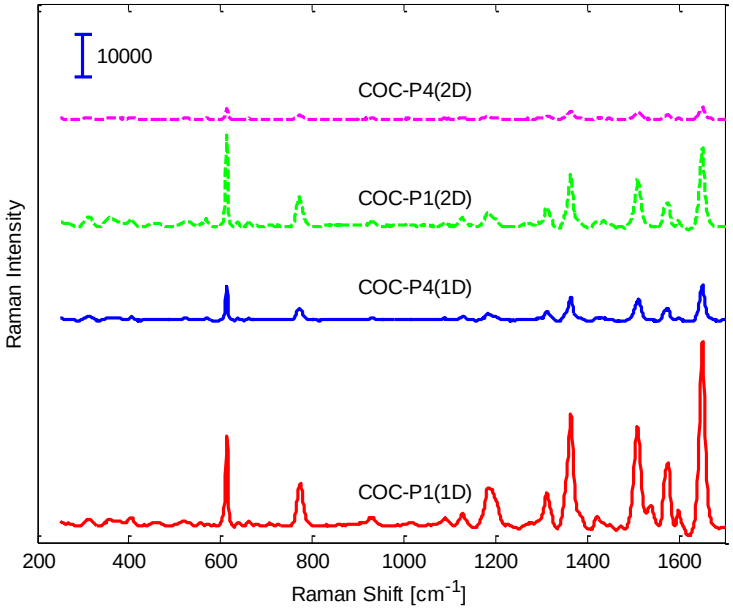


**Figure 21.** Raman spectra of Rh6G using fractions P1 and P4 for one dimensional (solid line) and two dimensional (dotted line) modifications on COC substrate.

Figure. 22 shows the variation in Raman peaks using error bars for fractions P1 and P4 for one and two dimensional nano-structures on the surface of COC. The silver colloidal solution fraction P1 produces large variations in the peak-to-peak Raman signal using one dimensional modulation as compared to the variations in signal produce by two dimensional modulations on COC substrate. It is because of the large size variations in silver nanoparticles and significant aggregation in fraction P1.

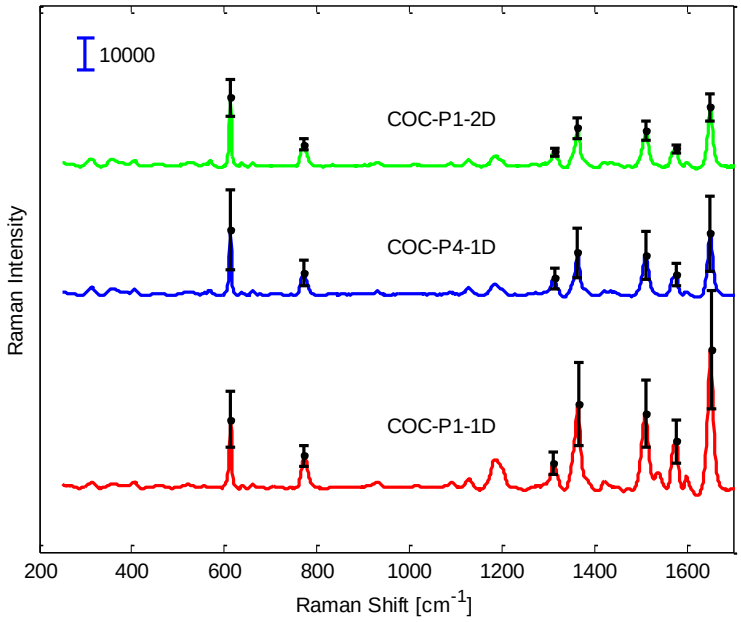


**Figure 22.** The variation in Raman peaks using error bar for one and two dimensional modulations on COC (Cyclo Olefin Copolymer) substrate using Ag colloidal fractions P1 and P4.

The distribution of silver nanoparticles can be seen in Fig. 23 on the modulated surface of COC substrate using fractions P1 and P2.

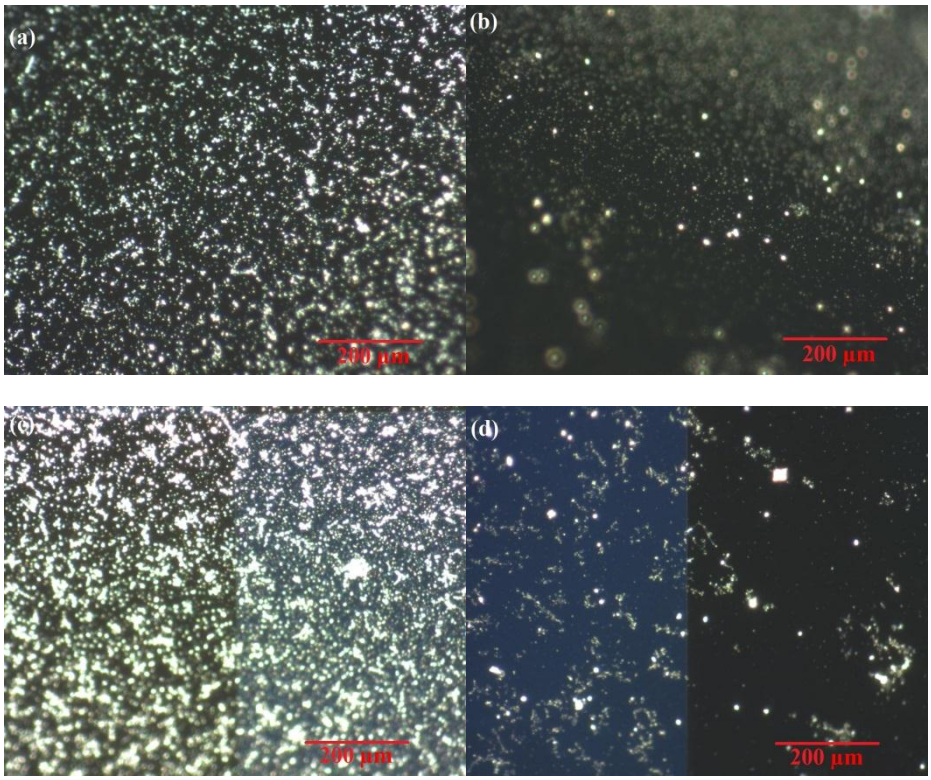


**Figure 23.** Microscope images of Ag particles distributions (a) P1 and (b) P4 for one dimensional modulation while (c) and (d) for two dimensional modulation.

## 5.4 CALCUALTION OF AVERAGE ENHANCEMENT FACTOR (AEF).

Generally the average surface enhancement factor is calculated using the following expression [48]:

$$AEF = \frac{I_{SERS}/c_{SERS}}{I_{RS}/c_{RS}}, \tag{12}$$

where $c_{RS}$ and $I_{RS}$ represent analyte solution concentration and the Raman signal produced by analyte solution under non-SERS conditions respectively, while $c_{SERS}$ and $I_{SERS}$ represent analyte concentration on the SERS substrate and the SERS signal from $c_{SERS}$ respectively. The Raman signal produced by analyte solution under non-SERS condition is very weak and difficult to observe in the spectrum. The Rh6G molecules Raman spectra have a quite high fluorescence and can be compared with Raman intensity to estimate the average enhancement factor. Under the same condition the normal Raman signal and fluorescence has a following relation [49]:

$$\frac{I_{RS}}{I_{FL}} = 10^{-9}, \tag{13}$$

In Eq. (13) $I_{FL}$ represents the fluorescence. Now using the Eq. (12) and considering the density of molecules per surface area is same for enhanced and non-SERS conditions, the enhancement factor can be calculated using relation

$$EF = \frac{I_{SERS}}{I_{FL}} \times 10^9. \tag{14}$$

In Fig. 24(a), the comparison of the enhancement factors for silver colloidal solutions prepared by Tollens and Citrate-reduced method is shown. The signal enhancement is 8-fold and 18-fold for PC and COC substrates respectively, due to the strong aggregation using Citrate-reduced silver colloidal solution as compared to the colloidal solution prepared by Tollens method.

The COC substrate for one dimensional modulated surface using a fraction P1 shows 4-fold more Raman signal enhancement in comparison with non-modulated COC substrate as it can be seen in Fig. 24(b). The silver colloidal fraction P1 shows high enhancement for one dimensional modulation corresponding to two dimensional modulations on COC substrate. Overall, one dimensional modulation shows high enhancement because fraction P1 contains variations in silver nanoparticles sizes, and also aggregated significantly more than two dimensional modulations.

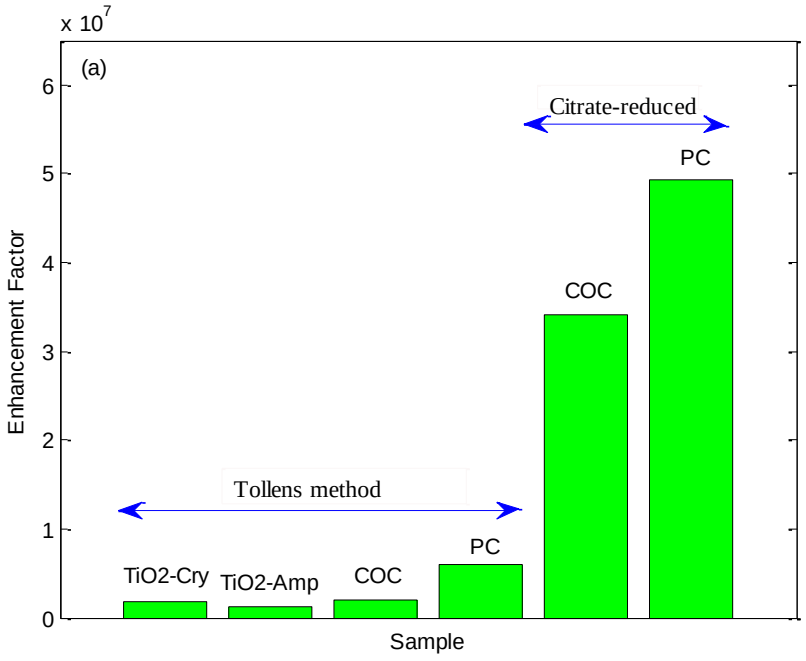

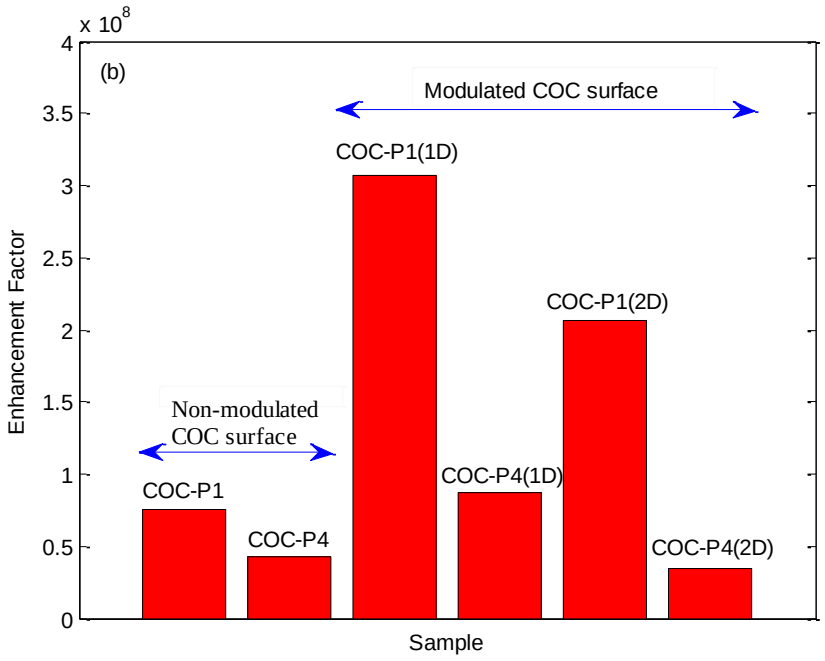


**Figure 24.** Comparison of enhancement factors for (a) Tollens and Citrate-reduced silver colloidal methods and (b) non-modulated and modulated COC substrate for colloidal fractions P1 and P4.

The Raman intensity was also measured by using silver, copper and silicon dioxide substrates, but these substrates produced a very weak signal. The $SiO_2$ films (10 nm) were coated on polymers to try for adjusting the surface chemistry for the Ag particles and used as substrates to analyze the Raman spectrum of Rh6G molecules, but because of the absorption through the film signal intensity was low. Transmission electron microscopy (TEM) images of the separated cluster of particles from the fractions P1 and P4 are shown in Fig. 25. Clearly, the fraction P1 contains a mixture of rods and balls of different sizes and many are in the form of aggregation which plays a significant role in the enhancement of the signal. The fraction P4 contains smaller particles with an average size of 40 nm.

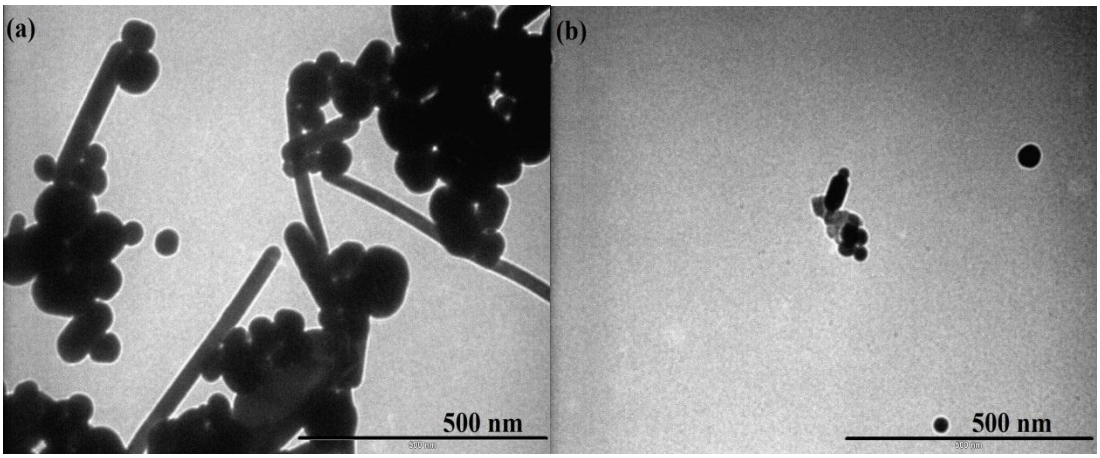


**Figure 25.**TEM images of Ag colloidal fractions (a) P1 and (b) P4

# *6. Conclusions*

On the basis of our SERS measurements we were able to find that silver colloidal solution prepared by Tollens method depicted uniform distribution on the surface of PC, COC and $TiO_2$ in amorphous and crystalline form. However, the Raman signal obtained was weak. The silver nanoparticles fabricated by Citrate-reduced colloidal solution method, agglomerated together giving high SERS signal. Silver colloidal solution distribution based on different particle sizes played a vital role to produce enhancement of signal and uniform surface area. The silver colloidal solution fraction with large variations in particles size produced a high signal. Depending on the distribution, sizes, and an aggregation of silver nanoparticles, polycarbonate (PC) and cyclo olefin copolymer (COC) acted as very effective substrates to produce SERS signal. The distribution of the reduced silver nanoparticles was more uniform on COC substrate than PC substrate. Concentration of silver nano-particles was dense on the edges of the PC and COC substrates which is most probable due to their hydrophobic nature. The periodical one and two dimensional modulations combined with reduced silver particles on the surface of COC material produced further enhancement in Raman signal. Silver nanoparticles were aligned and aggregated significantly on one dimensional modulation and produced high SERS signal. However, silver, copper and $SiO_2$ were not so effective materials in SERS measurements as they produced much fluorescence in the signal. The reduced silver particles combined with artificially modulated polymer substrates are promising in SERS measurements. However, further work on the surface chemistry is still required to produce even higher quality SERS substrates with high level uniformity, and it would be a good task for future work.

# *References*


[1] E. Le Ru and P. Etchegoin, *Principles of Surface Enhanced Raman Spectroscopy* (Oxford, UK, 2009).

[2] M. Fleischmann, P. J. Hendra, and A. J. McQuillan, "Raman spectra of pyridine adsorbed at a silver electrode", Chemical Physics Letters **26,** 163–166(1974).

[3] D. L. Jeanmaire and R. P. Van Duyne, "Surface Raman spectro electrochemistry Part I. Heterocyclic, aromatic, and aliphatic amines adsorbed on the anodized silver electrode", Journal of Electro analytical Chemistry and Interfacial Electrochemistry **84,** 1–20 (1977).

[4] M. G. Albrecht and J. A. Creighton, "Anomalously intense Raman spectra of pyridine at a silver electrode", Journal of the American Chemical Society **99,** 5215–5217 (1977).

[5] B. Sharma, R. R. Frontiera, A. Henry, E. Ringe, and R. P. Van Duyne, "SERS: Materials, applications and the future", Materialstoday **15,** 1–2 (2012).

[6] O. Lyandres, N. C. Shah, C. R. Yonzon, et al. "Real-time glucose sensing by surface-enhanced Raman spectroscopy in bovine plasma facilitated by a mixed decanethiol/mercaptohexanol partition layer", Analytical Chemistry **77,** 6134–6139 (2005).

[7] K. Chen, K. C. Vo-Dinh, F. Yan, et al. "Direct identification of alizarin and lac-dye on painting fragments using surface-enhanced Raman scattering", Analytica Chimica Acta **569,** 234–240(2006).

[8] K. Chen, M. Leona, K. C. Vo-Dinh, et al. "Application of surface-enhanced Raman scattering (SERS) for the identification of anthraquinone dyes used in works of art", Journal of Raman Spectroscopy **37,** 520–527 (2006).

[9] R. J. H. Clark, "Pigment identification on medieval manuscripts by Raman microscopy", Journal of Molecular Structure **347,** 417–444 (1995).

[10] H. Xu, E. J. Bjerneld, M. Kall, L. Borjesson, "Spectroscopy of Single Hemoglobin Molecules by Surface Enhanced Raman Scattering", Physics Review Letters **83**(21), 4357 (1999).

[11] T. Vo-Dinh, L. R. Allain, and D. L. Stokes, "Cancer Gene Detection using Surface-enhanced Raman Scattering (SERS)", J. Raman Spectroscopy **33,** 511–526 (2002).

[12] S. P. Mulvaney, M. D. Musick, C. D. Keating, and M, J. Nathan, "Glass-Coated, Analyte-Tagged Nanoparticles: A New Tagging System Based on Detection with Surface-Enhanced Raman Scattering", Langmuir **19**(11), 4784 (2003).

[13] C. R. Yonzon, C. L. Haynes, X. Zhang, J. T. Walsh, and R. P. Van Duyne, "A Glucose Biosensor Based on Surface-Enhanced Raman Scattering: Improved Layer, Temporal Stability, Reversibility, and Resistance to Serum Protein Interference", Analytical Chemistry **76,** 78 (2004).

[14] Y. C. Cao. J. Rongchao and C. A. Mirkin, "Nanoparticles with Raman Spectroscopic Fingerprints for DNA and RNA Detection", Science **297,** 1536 (2002).

[15] A. E. Grow, L. L. Wood, J. L. Claycomb, P. A. Thompson, "New Biochip Technology for Label-free Detection of Pathogens and their Toxins", Journal of Microbiological Methods **53,** 221 (2003).

[16] K. Kneipp, A. S. Haka, H. Kneipp, K. Badizadegan, N. Yoshizawa, C. Boone, K. E. Shafer-Peltier, J. T. Motz, R. R. Dasari, and M. S. Feld, "Surface-Enhanced Raman Spectroscopy in Single Living Cells using Gold Nanoparticles", Applied Spectroscopy **56**(2),150 (2002).

[17] K. Kneipp, H. Kneipp, V. B. Kartha, R. Manoharan, G. Deinum, I. Itzkan, R. R. Dasari, and M. S. Feld, "Detection and identification of a single DNA base molecule using surface-enhanced Raman scattering (SERS)",Journal of Physical Review E **57**, 6281–6284 (1998).

[18] S. Nie and S. R. Emory, "Probing single molecules and single nanoparticles by surface-enhanced Raman scattering", Science **275,** 11021–106(1997).

[19] K. Kneipp, Y. Wang, H. Kneipp, et al. "Single molecule detection using surface-enhanced Raman scattering (SERS)", Physical Review Letters **78,** 16671–670(1997).

[20] A.Kudelski, "Raman spectroscopy of surfaces", Surface Science **603,** 1328–1334 (2009).

[21] A. Taguchi1, N. Hayazawa, K. Furusawa ,H. Ishitobi, S. Kawata,"Deep-UV tip-enhanced Raman scattering", Journal of Raman Spectroscopy **40**(9), 1324–1330 (2009).

[22] P. Kukura, D. W. McCamant and R. A. Mathies, "Femtosecond Stimulated Raman Spectroscopy", Annual Review of Physical Chemistry **58,** 461–488 (2007).

[23] F. J. García-Vidal, and J. B. Pendry, "Collective theory for surface enhanced Raman scattering", Phyical Review Letters **77**(6), 1163–1166 (1996).

[24] N., Félidj, S. Lau Truong, J. Aubard, G. Lévi, J. R. Krenn, A. Hohenau, A. Leitnerand F. R. Aussenegg, "Gold particle interaction in regular arrays probed by surface enhanced Raman scattering", Journal of Chemical Physics **120**(15), 7141–7146 (2004).

[25] G. Laurent, N. Félidj, S. Lau Truong, J. Aubard, G. Levi, J. R. Krenn, A. Hohenau, A. Leitner, and F. R. Aussenegg, "Imaging surface plasmon of gold nanoparticle arrays by far-field Raman scattering", Nano Letters **5**(2), 253–258 (2005).

[26] G. Sauer, G. Brehm, S. Schneider, H. Graener, G. Seifert, K. Nielsch, J. Choi, P. Göring, U. Gösele, P. Miclea, and R. B. Wehrspohn, "In situ surface-enhanced Raman spectroscopy of monodisperse silver nanowire arrays", Journal of Applied Physics **97,**024308 (2005).

[27] Y. Lu, G. L. Liu, J. Kim, Y. X. Mejia, and L. P. Lee, "Nanophotonic crescent moon structures with sharp edge for ultrasensitive biomolecular detection by local electromagnetic field enhancement effect", Nano Letters **5**(1), 119–124 (2005).

[28] J. J. Baumberg, T. A. Kelf, Y. Sugawara, S. Cintra, M. E. Abdelsalam, P. N.Phillip and A. E. Russell, "Angle-resolved surface enhanced Raman scattering on metallic nanostructured plasmonic crystals", Nano Letters **5**(11), 2262–2267 (2005).

[29] V. K. Sharma, R. A. Yngard, Y. Lin, "Silver nanoparticles: Green synthesis and their antimicrobial activities", Advances in Colloid and Interface Science **145**, 83–96 (2009).

[30] C. V. Raman and K. S. Krishnan, "A new type of secondary radiation", Nature **121,** 501–502 (1921).

[31] A. Campion and P. Kambhampati,"Surface-enhanced Raman scattering," Chemical Society Reviews **27,** 241–250 (1998).

[32] D. P. Fromm, A. Sundaramurthy, A. Kinkhabwala, P. J. Schuck, G. S. Kino, and W. E. Moerner, "Exploring the chemical enhancement for surfaceenhanced Raman scattering with Au bowtie nanoantennas",The Journal of Chemical Physics **124,** 061101 (2006).

[33] O. Muskens, D. Christofilos, N. D. Fatti and F. Vall´ee, "Optical response of a single noble metal nanoparticle", Journal of Optics A: Pure and Applied Optics **8**, 264–272 (2006).

[34] S. A. Maier, *Plasmonics: Fundamentals and Applications* (Springer, New York, 2007).

[35] D. Pines, "Collective energy losses in solids", Reviews of Modern Physics **28,**184–199 (1956).
[36] P. L. Stiles, J. A. Dieringer, N. C. Shah, and R. P. Van Duyne, "Surface-Enhanced Raman Spectroscopy", Annual Review of Analytical Chemistry **1,** 601–26 (2008).
[37] M. Kerker and C. G. Blatchford, "Elastic scattering, absorption, and surface-enhanced Raman scattering by concentric spheres comprised of a metallic and a dielectric region", Physics Review B **26,** 4052(1982).
[38] E. J. Zeman and G. C. Schatz, "An accurate electromagnetic theory study of surface enhancement factors for silver, gold, copper, lithium, sodium, aluminum, gallium,indium, zinc, and cadmium", Journal of Physical Chemistry **91**(3), 634–643 (1987).
[39] J. Gersten and A. Nitzan, "Electromagnetic theory of enhanced Raman scattering by molecules adsorbed on rough surfaces", Journal of Chemical Physics **73,** 3023 (1980).
[40] G.C. Schatz and R.P. Van Duyne, "Image field theory of enhanced Raman scattering by molecules adsorbed on metal surfaces: Detailed comparison with experimental results", Surface Science **101,** 425–438 (1980).
[41] R. K. Chang and T. E. Furtak, *Surface-Enhanced Raman Scattering* (Plenum Press, New York, 1982).
[42] T. Vo-Dinh, "Surface-enhanced Raman spectroscopy using metallic nanostructures", Trends in Analytical Chemistry **17,** 8–9 (1998).
[43] A. Otto, I. Pockrand, J. Billmann and C. Pettenkofer, *The adatom model: how important is atomic scale roughness? In surface-enhanced Raman scattering* (Plenum Press, New York, 1982).
[44] C. Moser, L. Ho, E. Maye and F. Havermeyer, "Fabrication and applications of volume holographic optical filters in glass", Journal of Physics D: Applied Physics **41**, 224003(7pp) (2008).
[45] P. Hildebrandt and M. Stockburger, "Surface-enhanced resonance Raman spectroscopy of rhodamine6G adsorbed on colloidal silver", Journal of Physical Chemistry **88,** 5935–5944 (1984).
[46] O. Sllman, L. A. Bumm, R. Callaghan, C. G. Blatchford and M. Kerker, "Surface-enhanced Raman scattering by citrate on colloidal silver", Journal of Physical Chemistry **87**, 1014–1023 (1983).
[47] C. N. R. Rao, G. U. Kulkarni and P. J. Thomas, *Nanocrystals: Synthesis, Properties and Applications* (Springer, Berlin, 2007).
[48] E. C. Le Ru, E. Blackie, M. Meyer, and P. G. Etchegoin, "Surface enhanced Raman scattering enhancement factors: a comprehensive study," The Journal of Physical Chemistry **111** (37), 13794–13803(2007).
[49] J. Zhou, S. P. Xu, W. Q. Xu, B. Zhao, and Y. Ozaki, "In situ nucleation and growth of silver nanoparticles in membrane materials: a controllable roughened SERS substrate with high reproducibility," Journal of Raman Spectroscopy **40** (1), 31–37(2009).